



# A median based quadrilateral local quantized ternary pattern technique for the classification of dermatoscopic images of skin cancer

Varun Srivastava <sup>a</sup>, Deepika Kumar <sup>b</sup>, Sudipta Roy <sup>c,\*</sup>

<sup>a</sup> Department of Computer Science and Engineering, Thapar Institute of Engineering and Technology, Patiala, Punjab, India

<sup>b</sup> Department of Computer Science and Engineering, Bharati Vidyapeeth's College of Engineering, New Delhi, India

<sup>c</sup> Artificial Intelligence and Data Science, Jio Institute, Navi Mumbai, India



## ARTICLE INFO

### Keywords:

Medical imaging  
Image retrieval  
Image classification  
Texture detection

## ABSTRACT

Skin Cancer is one of the most widespread forms of cancer in the world which can be detected using dermatoscopic images. In this paper, a texture based feature extraction algorithm is presented for the classification of dermatoscopic images. A median based Local Ternary Pattern is extracted followed by the computation of local quantized ternary patterns. The feature set extracted is then classified using a modified convolutional neural network. The images used for the detection of multiple types of skin cancer are obtained from two publicly available datasets, HAM10000 and ISICUDA11. For the proposed technique, the average recall value, average precision and average accuracy is found to be 75.20%, 95.44% and 96% respectively. An average increase in accuracy for the proposed algorithm is up-to 50.6%, 24.1% and 4.7% over LTP, DLTerQEP and a DE ANN based algorithm respectively.

## 1. Introduction

Skin cancer is lethal if not detected in an early stage. This disease contributes for approximately 75% of the world's cancer. Mainly skin cancer is the abnormal growth of skin cells due to various reasons. One of the primary reasons could be exposure to ultra-violet sub-band of visible spectrum. Lesions are one of the main symptoms of skin cancer which can be analyzed to know if the lesion is due to abnormal growth of cells (cancer) or otherwise [1].

Many researchers worldwide have estimated that detection of skin cancer through traditional methods is much more invasive as compared to the automated detection. Further these procedures cannot determine melanoma at an early stage and also cannot distinguish between multiple types with enhanced precision. Thus detection of skin cancer using dermatoscopic images is a wide area of research and can contribute a lot to society if an efficient way can be proposed for the same. Existing classification methods are based on various feature extraction techniques; however, these do not ensure the best results. This research suggests integrating gradients with local binary patterns to further utilize the lesion segmentation mask's border-line properties (LBP) to enhance classification accuracy. These border-line properties are combined with conventional models in the suggested strategy to enhance the efficacy of skin lesion classification algorithms [2].

Many researchers have presented a variety of texture or shape based methods to extract features for the classification of skin cancer

\* Corresponding author.

E-mail address: [sudipta1.roy@jioinstitute.edu.in](mailto:sudipta1.roy@jioinstitute.edu.in) (S. Roy).

images. Some of the related work is summarized in following subsections.

### 1.1. Classification or retrieval techniques based on simple machine learning based classifiers

Authors in [3] presented a shape based approach for classification of dermatoscopic images having skin lesion. The skin cancer images are first pre-processed by using median filter for smoothing. Thereby image segmentation is done using Kernel Fuzzy C Means technique. Then nine features are extracted which are further refined using Red Fox Optimization (RFO) technique. This selected feature set is finally classified using a Multi-Layer Perceptron Model. In [4], a hybrid feature set is formed by using gray level co-occurrence matrix and Principal Component Analysis. The extracted feature set is further reduced using fuzzy C-Mean clustering. The feature set is finally classified using Support Vector Machines. The proposed method has been compared with state of the art techniques and has been found better in terms of specificity, sensitivity and accuracy. In [5], authors have computed the gradient in the image intensities of the neighbor pixels of a  $3 \times 3$  center pixel. The image is then binarized and its histogram is used as a feature vector. Also a color based feature vector is computed which is concatenated with texture based feature vector to form the final feature vector. Authors in [6] first segmented an image using Fuzzy C Mean Clustering from which Local Vector Patterns and LBP are then computed. A fuzzy classifier is thereby used for classification. The methodology has been compared with other state-of-the-art algorithms in terms of many metrics viz. sensitivity, specificity, F1 score, accuracy etc. A bag of features method is used along with Speeded-Up Robust Features to classify the lesion image as cancerous/non-cancerous [7]. Authors in [8] elucidated fuzzy c-means segmentation to extract cancer-affected region, then Firefly optimization has been used for extracting the dominant feature. The extracted dominant feature reduced the error rate by highest gradient. The performance is then compared with state-of-the-art algorithms. Authors in [9] first extracted the lesion-affected region by using watershed segmentation followed by extraction of features like shape, ABCD rule, and GLCM. These features are then fed into kNN (k Nearest Neighbour), RF and SVM for further classification. SVM proved to be superior to other two. In [10], authors have proposed a novel genetic programming (GP) technique for the classification of dermatoscopic images. The algorithm was based on extraction of Local Binary Pattern (LBP) features by GP which increased the performance over simple LBP features and other related feature vectors.

### 1.2. Classification or retrieval techniques by deep learning based classifiers

In [11], Out of Distribution (OOD) dataset is created from Skin Archive Munich dataset. The robustness included is thereby used for classification using deep networks. The algorithm proved to be better than many state-of-the-art methods. The proposed technique achieved up to 85.7% accuracy. In [12], authors claimed to achieve sensitivity and specificity values at par with those obtained from dermatologists. An advanced deep learning technique has been used to train 12,378 open-source dermatoscopic images obtained from ISIC image archive and HAM10000 dataset. Authors have generated a34-layer residual network in [13] which is trained on three benchmark pigmented lesions dataset. The datasets used are from ISIC archive, HAM 10,000 and Harvard data-verse. The authors have proved that clinicians along with AI based support can give much better results as compared to standalone AI approach or clinicians. Also AI based approaches are better when multiclass classification has to be performed. The mean recall achieved was 77.7%, with an accuracy of 80.3%.

In [14], the proposed algorithm pre-processes the images from three publicly available datasets and then enhances the images further by using a faster- Region based CNN to obtain a feature vector. Thereby Fuzzy K-Means (FKM) clustering is applied for segmentation of the melanoma affected region in the dataset images. The algorithm is used over ISBI-2016, ISIC-2017 and PH2 datasets and the algorithm outperformed related state of the art approaches. Brinker et al. [15] used Res-Net model for the classification of dermatoscopic images and achieved a sensitivity of up to 74.1% and specificity of around 60.0%. Authors proposed deep learning architectures which were mainly comprised of layers from the architecture of InceptionV3 and ResNet50 and used them to classify 7895 dermatoscopic images [16]. A Mobile-Net model trained on around 1280,000 images was used over HAM10000 dataset in [17]. The Mobile-Net model is fine-tuned over 10,015 dermatoscopic images for better accuracy.

Authors in [18] trained 11 different Convolutional Neural Networks (CNNs) over HAM10K dataset. The performance of Dense-Net169 has been found to be best with an accuracy of around 92.25%. Also, the model has been tested on mobile device cameras. In [19], authors used Google-Net to classify eight different types of skin lesions. The accuracy, sensitivity, specificity, and precision obtained were 94.92%, 79.8%, 97%, and 80.36% respectively to classify between eight different classes of skin lesions. In [20], authors performed multi-classification on skin lesions utilizing HAM10000 dataset. This comparative analysis used different transfer learning models viz. VGG19, inceptionV3, InceptionResNetV2, ResNet50, Xception and Mobile-Net for classification. XceptionNet has outperformed as compared to all other models and achieved an accuracy of 90.48%. As clearly seen from [2] and [13], AI based automated approaches gives better results than manual classification for classification of skin cancer images when multi-class classification needs to be done. In the presented work, since multi-class skin lesion classification needs to be done, therefore automated approach using deep learning models and texture based features is used.

**Key Contribution:** Many texture-based features have been used by the researchers in the past for classification of skin cancer images. However, many techniques were only able to classify between the cancerous and non-cancerous cells. They were not able to classify between various types of skin cancers or abnormal mass growth of skin cells. Also, the presence of noise in the images has not been effectively dealt with. The proposed mechanism classifies various types of dermatoscopic images with skin cancer from lesion or abnormal growth of skin cells using texture based features and outperforms the existing related techniques. The noise is also removed while computing the texture by use of median value for computing the threshold of Local Ternary Pattern (LTP). Further, in the given work the LTP is extracted by using  $7 \times 7$  neighborhoods and by using median threshold. Using a bigger neighborhood yields a more

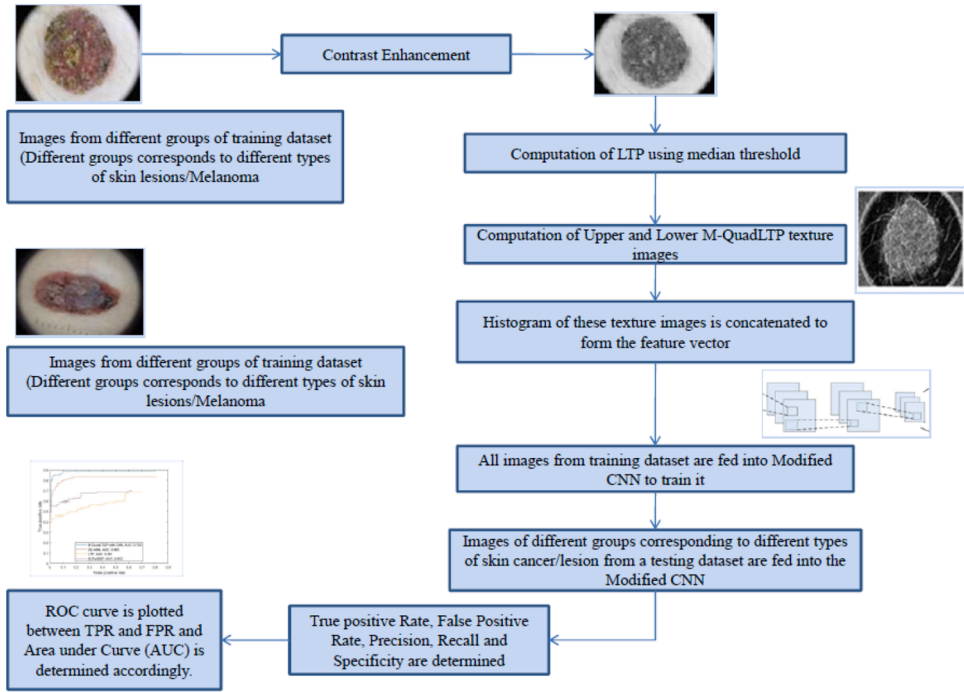


**Fig. 1.** A flowchart of the experimental set-up used to compare proposed methodology along with other techniques.

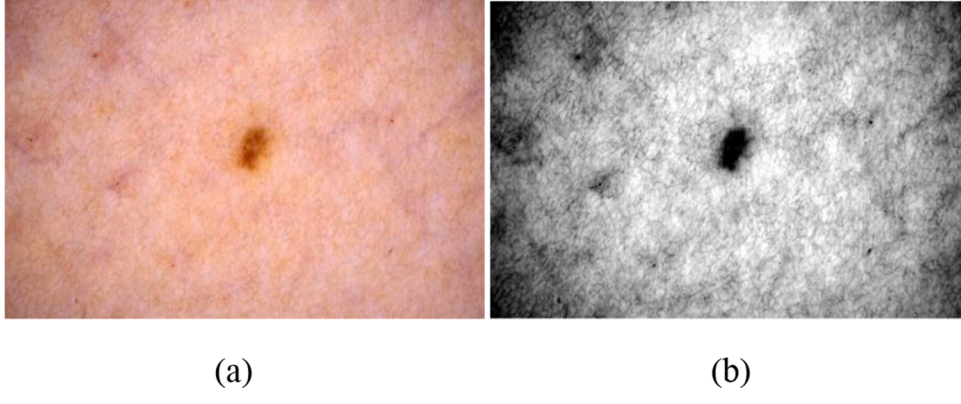


**Fig. 2.** (a) Original Image (b) Image obtained after contrast enhancement.

powerful feature vector along with lesser noise due to median based threshold. Thereby the results are better as compared to recent related texture based algorithms. Also, because of the use of a simplistic architecture of modified Convolutional neural network, the time taken by the algorithm is reduced drastically as compared to the existing deep learning based models. There are seven types of skin cancer in one dataset and nine different types of skin cancer in another. All the images have been classified into their respective group. The performance in terms of accuracy, precision, specificity and recall has been computed and is found to be better than related state of the art techniques.

The paper has been organized in the following manner. [Section 2](#) describes the proposed methodology used for the detection of various types of skin cancers. [Section 3](#) presents the results and comparison of the proposed mechanism with state of the art techniques and [Section 4](#) concludes the paper.

## 2. Methodology

The proposed work involves image pre-processing and extraction of texture based features from two publicly available datasets. Thereby a modified Convolutional Neural Network (CNN) is used for classification of these feature vectors. The extraction of feature vectors and classification using CNN is explained in further subsections. A detailed experimental flow of the proposed work is shown in

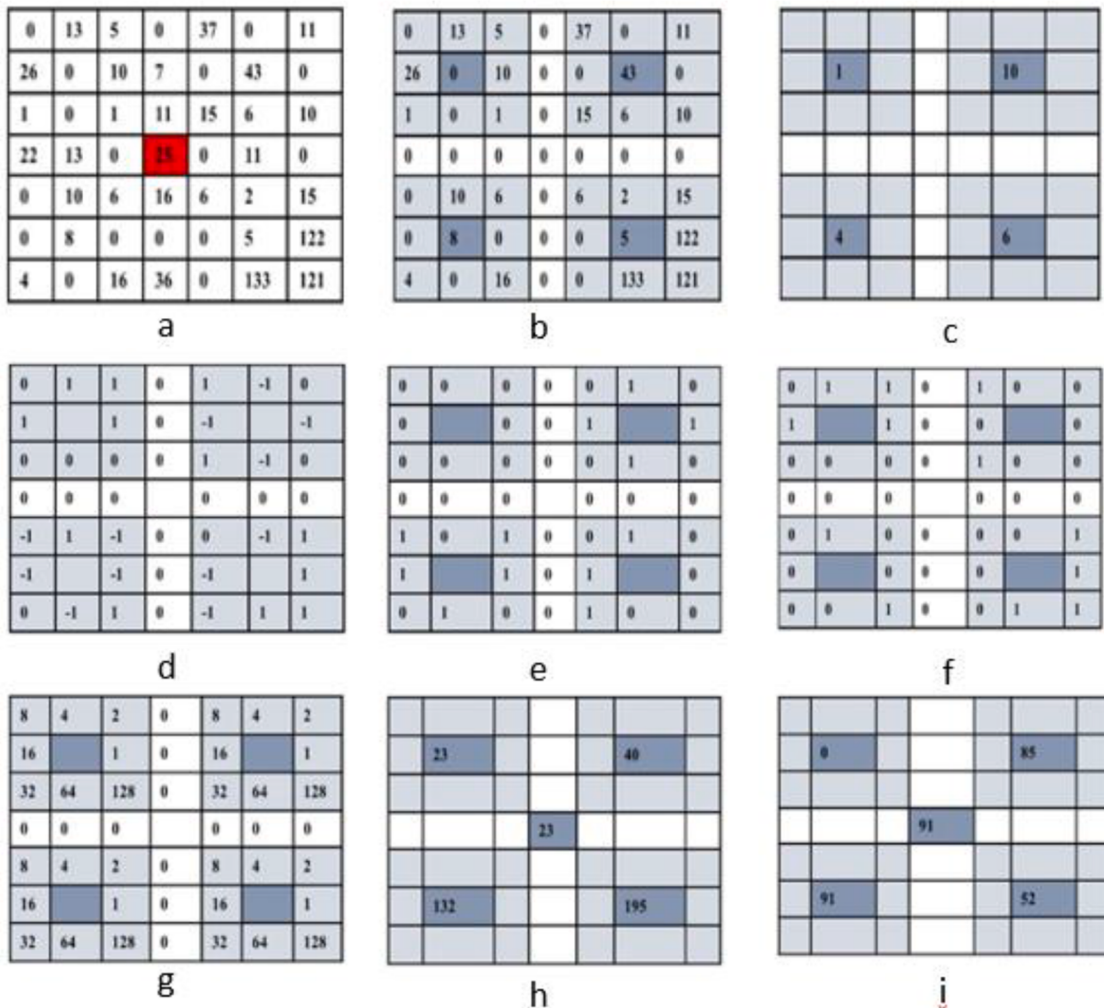


**Fig. 3.** (a)  $7 \times 7$  image grid extracted from an original image (b) Grid prepared for the extraction of M-QuadLTQP features (c) Median values used to compute threshold for each quadrant (d) M-QuadLTP values computed for each quadrant (e) Upper M-QuadLTP values for a given central pixel (f) Lower M-QuadLTP values for a central pixel (g) Weight vector (h) Final Upper M-QuadLTQP value for a central pixel (i) Final Lower M-QuadLTQP value for a central pixel.

**Fig. 1.**

#### A. Data Acquisition

Images from two publicly available datasets viz. HAM10000 repository [21] and ISIC\_UA-1 repository [22] are used for extraction of feature vectors and classification of skin cancer images. These two repositories have dermatoscopic images taken from different parts of the body and divided into various classes of skin cancer or lesion. HAM10000 images are divided into seven different classes of skin cancer whereas ISIC\_UA-1 dataset is divided into nine different classes of skin cancer.

HAM10000 has 10,000 images that are collected from different populations and are stored as different modalities. All the images are standardised for classification by a neural network model to a dimension of  $800 \times 600$ . The ISIC\_UA-1 dataset has 2357 images of skin cancer derived from different populations and the images are available in Digital Imaging and Communications in Medicine (DCM) as well as Joint Photographic Experts Group (JPEG) format of size  $1024 \times 768$ .

#### B. Pre-processing of images

The dermatoscopic images from the dataset are first converted to corresponding greyscale images. Then the contrast enhancement is done so that 1% of the input data will get saturated at the low and high pixel intensities of the input image. The Contrast enhancement for a random sample of ISIC\_UA-1 dataset image is shown in Fig. 2.

#### C. Feature extraction

The feature extraction is done by following steps:

##### (i) Grid Preparation

To extract the feature set of Median based Quadrilateral Local Ternary Quantized Pattern (M-QuadLTQP) from an original image, the relationship between neighbor pixels of a center pixel is explored. This is done by considering pixels in  $7 \times 7$  neighbourhood grid of

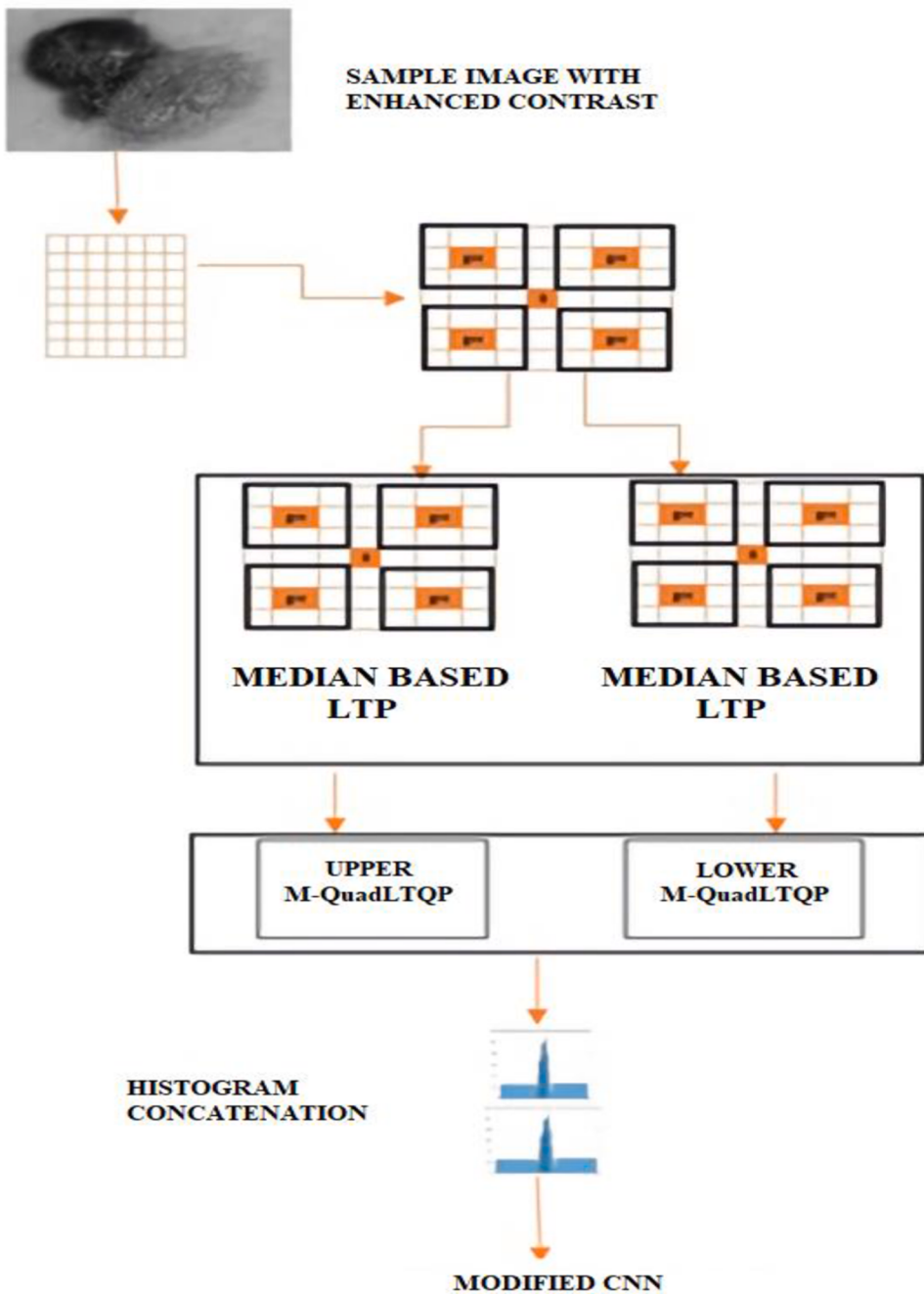


**Fig. 4.** Schematic representation for image retrieval using M-QuadLTQP feature extraction.

a center pixel (pixel with pixel intensity 25 in Fig. 3(a)). Each pixel of the original image is considered as a center pixel and the corresponding M-QuadLTQP values are computed for it. To compute this, for a center pixel, the surrounding  $7 \times 7$  neighbourhood grid is divided into four quadrants of  $3 \times 3$  pixels as shown in Fig. 3(b). In [23], Deep et al. have demonstrated that a texture image obtained by processing a  $7 \times 7$  neighbourhood yields better results as compared to a  $3 \times 3$  or any other neighbourhood.

#### (ii) Extraction of Dynamic Local Ternary Pattern (LTP)

A Dynamic LTP is then computed for each  $3 \times 3$  sub-matrix of the grid obtained in the previous subsection using eq. (1). To compute the Dynamic LTP, first a median value of each  $3 \times 3$  pixel quadrant is computed. Thereby, four median values are computed as shown in Fig. 3(c) corresponding to each quadrant of Fig. 3(b). The median value is chosen so as to remove the salt and pepper noise if present. The two thresholds are taken that are 't' units apart from the median value. Hence for the first quadrant, since the median value is 1, so the thresholds are -1 and 3. Similarly for second, third and fourth quadrant, the thresholds are 8 and 12, 2 and 6, and 4 and 8

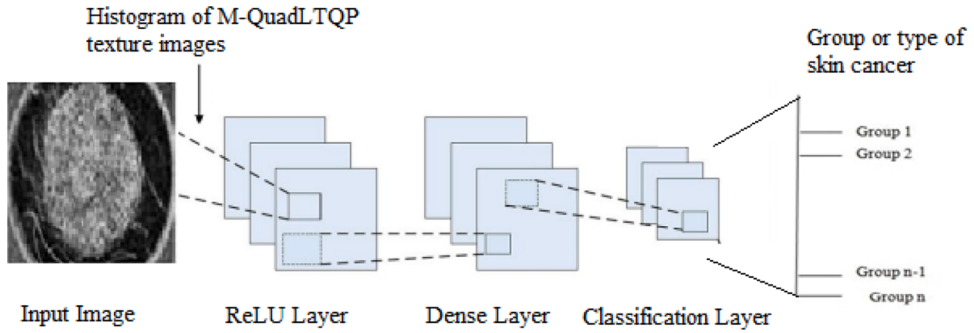


**Fig. 5.** A Modified-CNN (M-CNN) architecture used in the classification of M-QuadLTQP features extracted from the dermatoscopic images.

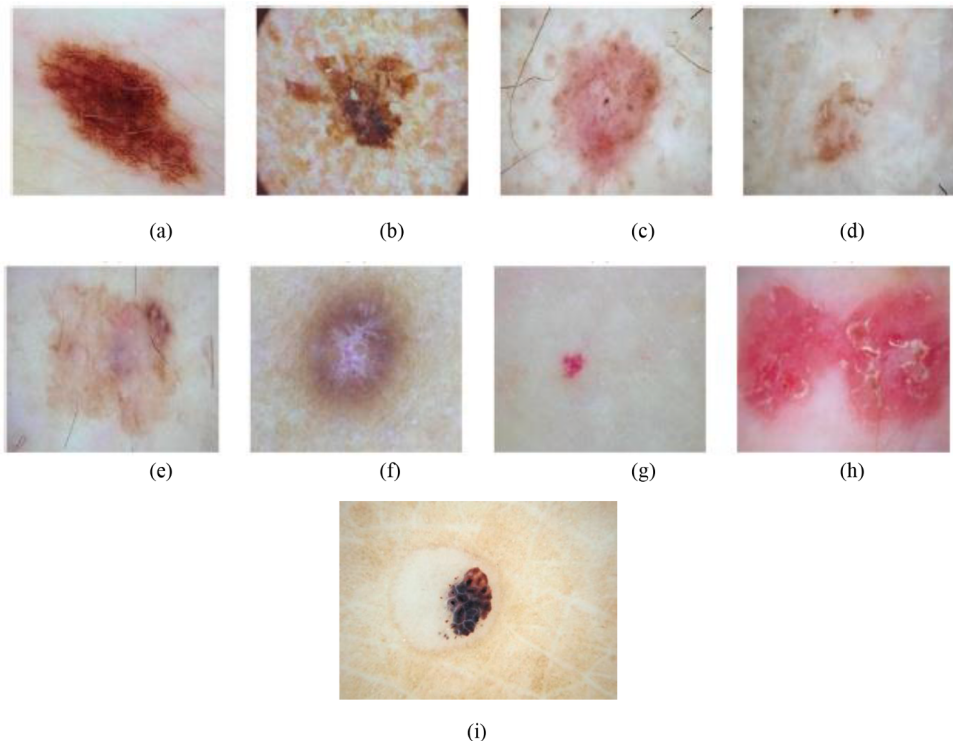


**Fig. 6.** Different types of dermatoscopic skin lesions like (a) Nevus (b) Melanoma (c) Basal Cell Carcinoma (d) Actinic Keratosis (e) Benign Keratosis (f) Dermatofibroma (g) Vascular Lesion (h) Squamous Cell Carcinoma (i) Seborrheic keratosis.

respectively. Here  $t$  is chosen as 2.

$$f(x, g_m, t) = \begin{cases} +1 & \text{if } x \geq g_m + t \\ 0 & \text{if } |x - g_m| < t \\ -1 & \text{if } x \leq g_m - t \end{cases} \quad (1)$$

Here  $x$  is the neighbourhood pixel of the central pixel;  $g_m$  is the pixel intensity of the median pixel in corresponding  $3 \times 3$  quadrant. Each value in a quadrant is compared with the respective upper threshold ( $g_m + 2$ ) and lower threshold value ( $g_m - 2$ ) using eq. (1). The values that are above the higher threshold value are replaced with 1 and the values below lower threshold are replaced with -1. The values that are between upper and lower threshold values are replaced with 0. The values obtained after computing Dynamic LTP are shown in Fig. 3(d).

### (iii) Computation of Lower and Upper M-QuadLTP

For each  $3 \times 3$  matrix of every quadrant in Fig. 3(d), two matrices are obtained, one by considering all positive values and labeling them 1, and second by considering all negative values and labeling them 1, while keeping remaining values as zero. The matrix obtained by considering all positive values is termed as upper M-QuadLTP matrix and the matrix obtained by considering negative values is termed as lower M-QuadLTP matrix. Thus, two  $7 \times 7$  matrices from matrices in Fig. 3(d) are obtained. These are given in Fig. 3(e)

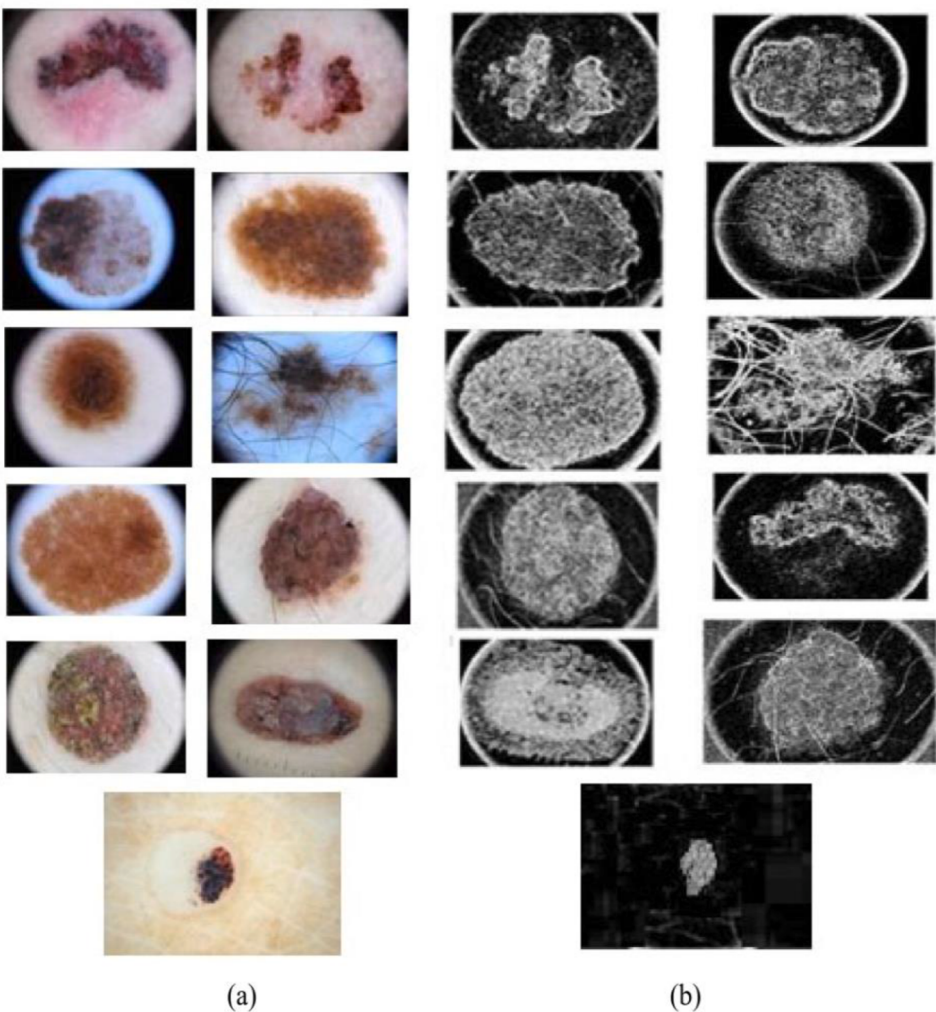


**Fig. 7.** (a) Original skin cancer images from 9 different groups of ISIC\_UDA dataset (b) Corresponding M-QuadLTQP images obtained.

and Fig. 3(f). A dot product of weight vector given in Fig. 3(g) is then calculated with matrices of Fig. 3(e) and Fig. 3(f). The product is summed up to obtain four values for Upper and Lower M-QuadLTQP matrices.

#### (iv) Calculation of Final M-QuadLTQP values

The four values obtained after summing up the weighted upper and lower M-QuadLTQP matrices are shown in Fig. 3(h) and Fig. 3(i). Finally, two M-QuadLTQP values are obtained from these two matrices by considering the lowest value from Upper M-QuadLTQP and highest value from Lower M-QuadLTQP. These values as shown in Fig. 3(h) and Fig. 3(i) are 23 and 91 respectively. Thus, each central pixel is replaced by two M-QuadLTQP values and this procedure is repeated for all the pixels in the image.

Hence two texture images with M-QuadLTQP values are obtained for each image in the database. The histogram of these two images are concatenated and then used as a feature vector for classification or retrieval of similar images. A complete schematic representation of the steps used in feature extraction is given in Fig. 4.

#### D. Classification using modified CNN

A modified CNN is then used for classification of the features thereby extracted. The modified CNN used in the proposed methodology is a single layer CNN network comprised of Rectified Linear Unit (ReLU) layer, Dense Layer and Classification layer. Since the features are fed directly into the CNN, thus convolutional layer is dropped. Also, on adding Max pooling layer the performance was degrading since it was decreasing the size of feature vectors, thereby Max pooling layer is also discarded. Further on adding more parallel layers, there was no increase in the precision and recall values and thus a simplistic single layered architecture has been used. Fig. 5 presents the architecture used for the classification.

### 3. Results and discussions

The proposed algorithm is implemented on a computational drive of 2.0 GHz, 12GB RAM and on MATLAB platform.

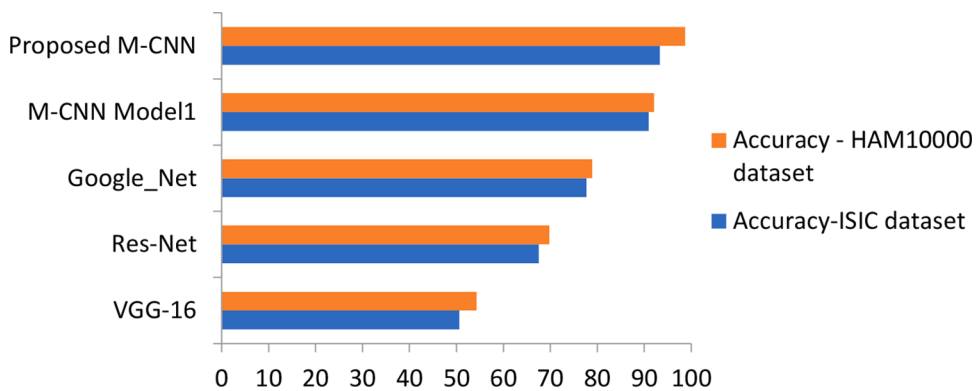


**Fig. 8.** Accuracy with respect to different CNN architectures when trained on M-QuadLTQP feature vector for ISIC\_UDA-1 data.

The datasets used are dermatoscopic images with different types of skin cancer and simple lesions from ISIC\_UDA-1 [22] and from HAM10000 [21] repository. The ISIC\_UDA-1 dataset had images of nine different types of skin cancer or precancerous lesion (or keratosis) viz. Nevus, Melanoma, Basal Cell Carcinoma, Actinic Keratosis, Benign Keratosis, Dermatofibroma, Vascular Lesion, seborrheic keratosis and Squamous Cell Carcinoma. The dataset has 2357 images in total of .jpg format. The resolution of each image is  $1024 \times 768$ . The HAM10000 dataset has seven types of images for seven different types of skin cancer or precancerous images namely Nevus, Melanoma, Basal Cell Carcinoma, Actinic Keratosis, Benign Keratosis, Dermatofibroma, and Vascular Lesion. There are a total of 10,015 images of .jpg format. The resolution of each image is  $800 \times 600$ . The images belonging to nine different groups of skin cancer or lesion from ISIC\_UDA dataset are shown in Fig. 6.

After applying M-QuadLTQP, the corresponding texture images obtained are shown in Fig. 7 for images from ISIC\_UDA-1 dataset. To compute the efficacy of standalone M-QuadLTQP features, the Euclidean distance between feature vector extracted from the query image and all the images of the database are computed. A threshold value of Euclidean distance is thereby set to classify the images. This threshold value of Euclidean distance is set in a manner so that Average Retrieval Rate (ARR) value is maximized.

Also, the extracted feature set has been used to train a CNN model given in section 2(d). The feature vectors are fed into the modified CNN comprised of ReLU layer, dense layer and a classification layer. The model is thereby trained for the proposed feature set. Further metrics like accuracy, recall, precision, specificity, Receiver Operating Characteristics Curve (ROC) and (Area Under Curve) AUC value are computed. Three state of the art algorithms viz. Local Ternary Pattern (LTP) [24], Directional Local Ternary Quantized Extrema Pattern (DLTerQEP) [23] and Differential Evolution (DE) – Artificial Neural Network (ANN) inspired Skin Cancer Detection Approach Using Fuzzy C-Means Clustering (FCMC) [25] are compared with the given work using these metrics computed using Eq. (2) to Eq. (6). The results are also compared in terms of accuracy which can be calculated using Eq. (6).

The use of a simplistic Modified CNN (M-CNN) is justified in Fig. 8. When the feature set was trained on popular CNN classification models like VGG-16, Google-Net and Res-Net, the accuracy obtained on these models has been found to be less than state of the art algorithms. This is due to the fact that these models extract features by their convolutional layer whereas in the proposed work the features based on skin cancer has been extracted already and are fed for training the network. Thereby a Modified CNN Model is proposed where in Convolutional layer is dropped from VGG-16 model. The model is referred to as M-CNN Model 1 and the accuracy improved as shown in Fig. 8. The model has been further modified by keeping single layer architecture and by dropping max-pooling layer to form the proposed M-CNN model. This led to further improvement in the accuracy and reduction in the complexity of the network. The corresponding results obtained for different values of accuracy for different CNN models are summarized in Fig. 8.

ARP and ARR can be computed using Eq. (2) and Eq. (4). If there are total 'n' classes in the output, then

$$\text{ARP} = \frac{\sum_{i=0}^n P(i)}{n} \quad (2)$$

where  $P(i)$  is the Precision of  $i^{\text{th}}$  class given as

$$P(i) = \frac{TP(i)}{TP(i) + FP(i)} \quad (3)$$

Here  $TP(i)$  is the number of true positive samples for  $i^{\text{th}}$  class and  $FP(i)$  is the number of False Positive samples for the  $i^{\text{th}}$  class. Similarly,

$$\text{ARR} = \frac{\sum_{i=0}^n R(i)}{n} \quad (4)$$

where  $R(i)$  is the Recall or Sensitivity of  $i^{\text{th}}$  class given as

$$R(i) = \frac{TP(i)}{TP(i) + FN(i)} \quad (5)$$

**Table 1**

Performance of M-QuadLTQP in terms of Sensitivity, Specificity and Precision for various algorithms on ISIC-UDA-1 dataset.

S. No.	Type of skin cancer	LTP [24]	DLTerQEP [23]	DE-ANN based algorithm using FCMC [25]	M- QuadLTQP	M-QuadLTQP with Modified CNN	
1	Group 1	Precision	70.32	78.63	81.26	82.47	
		Specificity	60.60	82.30	70.70	80.70	
		Sensitivity	46.54	48.23	51.26	50.25	
2	Group 2	Precision	67.83	77.52	78.94	79.40	
		Specificity	59.72	84.55	65.80	80.10	
		Sensitivity	65.63	66.35	65.34	66.66	
3	Group 3	Precision	71.54	81.63	89.28	91.24	
		Specificity	58.30	78.49	67.12	76.70	
		Sensitivity	72.32	70.43	73.44	75.24	
4	Group 4	Precision	69.84	82.30	91.19	92.35	
		Specificity	62.50	79.90	70.60	79.90	
		Sensitivity	68.41	72.16	74.83	75.73	
5	Group 5	Precision	62.45	73.45	89.75	87.87	
		Specificity	65.40	75.71	67.90	81.80	
		Sensitivity	74.66	75.84	76.82	75.85	
6	Group 6	Precision	70.92	76.56	87.66	89.53	
		Specificity	66.50	80.84	68.60	79.40	
		Sensitivity	73.27	79.55	80.84	83.66	
7	Group 7	Precision	71.26	78.66	85.24	87.66	
		Specificity	62.80	80.90	69.90	82.10	
		Sensitivity	65.08	66.52	74.65	75.47	
8	Group 8	Precision	77.93	85.68	94.23	95.44	
		Specificity	59.40	75.60	66.06	77.80	
		Sensitivity	67.29	66.65	74.86	75.14	
9	Group 9	Precision	78.64	84.55	91.16	93.48	
		Specificity	64.72	81.49	71.26	82.40	
		Sensitivity	65.45	67.86	73.84	74.53	
Average RP		71.19	79.88	87.63	88.82	93.17	
Average Specificity		62.22	79.99	68.66	80.10	81.22	
Average RR		66.51	68.17	71.76	72.50	74.47	

Here FN(i) is the number of False Negative samples for i<sup>th</sup> class.

$$\text{Further, Specificity} = \frac{TN(i)}{TN(i) + FP(i)} \quad (6)$$

Here TN(i) is the number of true negative samples for a class i.

$$\text{Accuracy} = \frac{\text{Number of images correctly classified to their respective class}}{\text{Total number of images in the database}} \times 100 \quad (7)$$

### 3.1. Experiment 1: ISIC\_UDA-1 dataset

The dataset had nine different types of skin cancer or lesion based dermatoscopic images. The precision and recall for each type or group has been computed for M-QuadLTQP features. For standalone M-QuadLTQP features, a threshold value of Euclidean distance is used to retrieve similar images. The threshold is decided based on the value giving maximum ARR and ARP values when compared with expected value of the output class. Also, the M-QuadLTQP features are trained on a modified-CNN model. As seen from Table 1, the precision and recall values for all groups when M-QuadLTQP is trained on CNN model is better than LTP [24], DLTerQEP [23] and DE-ANN based approach [25]. The precision and recall values for M-QuadLTP features are less in Group 5 than DE-ANN based approach when CNN is not used. However as seen from Table 6, the M-QuadLTQP features take lesser time to retrieve similar images for a query image as compared to DE-ANN based algorithm. Further, CNN based model has improved the ARR by 2.7% and ARP by 4.89%. The ARR and ARP values of three state art of the algorithms viz. basic LTP technique, a similar texture based Directional Local Ternary Quantized Extrema Pattern (DLTerQEP) algorithm and a state of the art technique having DE-ANN classifier using Fuzzy C means along with M-QuadLTQP features for ISIC\_UDA-1 dataset are given in Table 1.

It can be seen clearly from Table 1 that the proposed method when used along with modified CNN is performing better than the related state of the art algorithms. There has been an improvement of 3.77%, 9.2% and 11.9% in terms of recall for the proposed methodology when compared with DE-ANN based algorithm using FCMC [25], DLTerQEP [23] and LTP [24] method. Also, the precision values obtained on ISIC data are compared in Table 3. Further, Table 3 shows that M-QuadLTQP outperformed LTP, DLTerQEP and DE-ANN algorithm in terms of precision for all groups/types of skin cancer. The percentage improvements in precision values are 6.3%, 16.63% and 30.9% respectively over DE-ANN, DLTerQEP and LTP algorithm.

In terms of Specificity also, M-QuadLTQP outperforms all other state of the art algorithms as seen from Table 1. The percentage improvement is 18.29%, 1.53% and 30.5% respectively over DE-ANN, DLTerQEP and LTP algorithms. A Receiver Operating

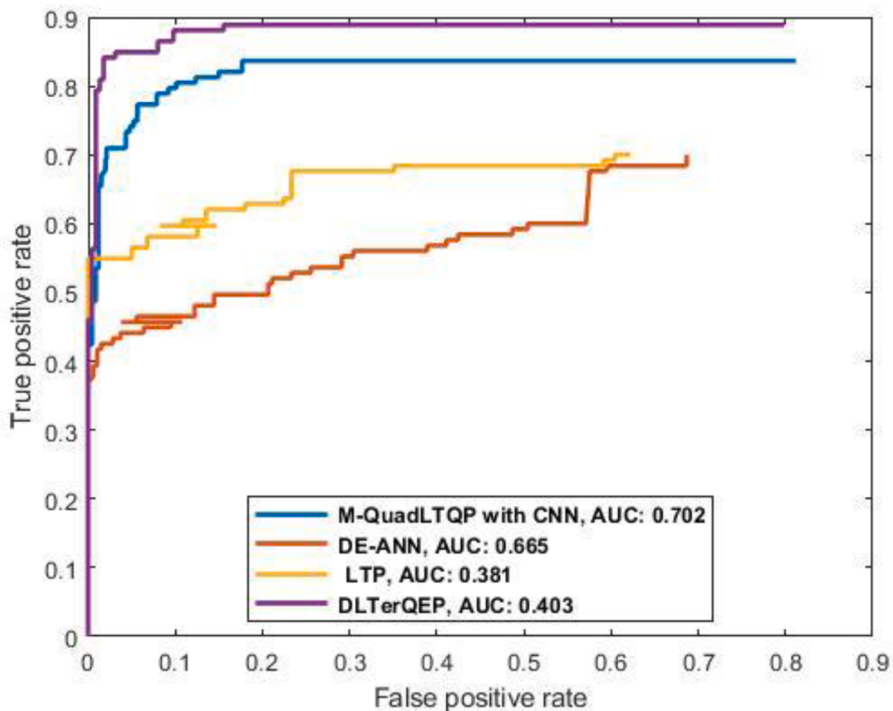


**Fig. 9.** A ROC curve and corresponding AUC values for ISIC UDA-1 dataset.

**Table 2**

Performance of M-QuadLTQP in terms of Sensitivity, Specificity and Precision for various algorithms on HAM10000 dataset.

S. No.	Type of skin cancer	LTP [24]	DLTerQEP [23]	DE-ANN based algorithm using FCMC [25]	M- QuadLTQP	M-QuadLTQP with Modified CNN	
1	Group 1	Precision	69.85	74.54	95.54	96.34	
		Specificity	59.30	89.70	93.40	94.70	
		Sensitivity	44.25	49.37	52.45	53.45	
2	Group 2	Precision	65.66	73.46	95.56	95.66	
		Specificity	62.15	91.90	92.10	92.90	
		Sensitivity	55.77	57.18	66.77	68.68	
3	Group 3	Precision	73.27	87.23	95.36	96.58	
		Specificity	59.90	80.90	90.30	92.70	
		Sensitivity	61.28	64.69	69.29	73.29	
4	Group 4	Precision	68.08	83.47	99.24	99.57	
		Specificity	64.30	95.91	99.32	99.75	
		Sensitivity	56.79	59.25	72.16	74.86	
5	Group 5	Precision	62.16	72.53	99.73	99.39	
		Specificity	61.69	93.01	96.72	92.90	
		Sensitivity	63.10	72.07	79.14	78.24	
6	Group 6	Precision	69.44	73.85	97.66	98.00	
		Specificity	65.40	96.25	97.67	99.65	
		Sensitivity	62.86	71.36	78.27	77.86	
7	Group 7	Precision	69.53	79.24	92.72	92.77	
		Specificity	60.80	90.10	93.11	94.50	
		Sensitivity	61.33	63.84	76.58	81.23	
Average RP		68.28	77.76	96.54	96.90	97.71	
Average Specificity		61.93	91.11	94.66	95.30	98.66	
Average RR		57.91	62.53	70.66	72.51	75.93	

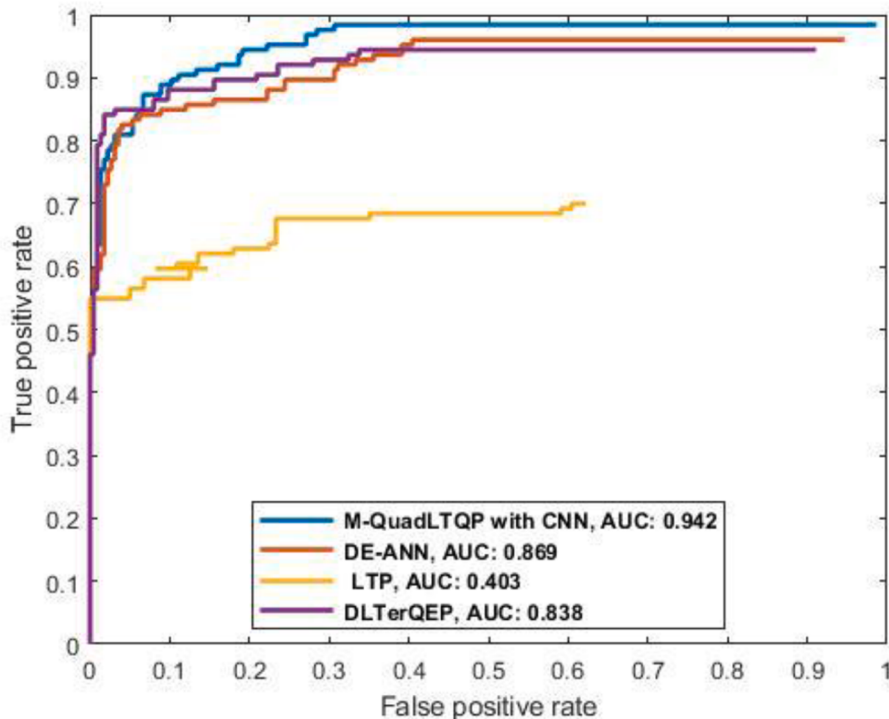
Characteristics (ROC) curve is plotted between True Positive Rate (TPR) and False Positive Rate (FPR) values obtained for ISIC\_UDA-1 dataset as given in Fig. 9. The ROC curve for proposed M-QuadLTQP is found to be better as compared with LTP, DLTerQEP and DE-ANN using FCMC algorithm. Further the AUC value is highest for the proposed work. The maximum value for TPR is found to be 0.888 whereas the maximum value for FPR was found to be 0.799.

The corresponding AUC values calculated are 0.702, 0.66, 0.381 and 0.403 for M-QuadLTQP, DE-ANN, LTP and DLTerQEP algorithms respectively.

**Table 3**

Performance Comparison in terms of accuracy for both datasets.

S. No.	Database	LTP [24]	DLTerQEP [23]	DE-ANN based algorithm using FCMC [25]	M-QuadLTQP	M-QuadLTQP with Modified CNN
1	ISIC UDA-1	62.35	75.78	86.40	89.50	93.30
2	HAM10000	65.18	78.90	96.92	97.80	98.70
	Average value	63.76	77.34	91.66	93.65	96.00

**Fig. 10.** ROC curve and corresponding AUC values for different algorithms in the case of HAM10000 dataset.

### 3.2. Experiment 2: HAM10000 dataset

The three algorithms viz. LTP, DLTerQEP and DE-ANN based approach are compared to the M-QuadLTQP technique on HAM10000 dataset in terms of ARP, ARR, specificity and accuracy. There are seven different groups in HAM10000 dataset corresponding to seven different types of skin cancer or lesion images. The sensitivity, specificity and precision values for these seven groups are summarized in Table 2. As observed from Table 2, the recall and precision values for group 5 is higher for DE-ANN as compared to standalone M-QuadLTQP feature vector. However, this decrease in recall can be justified with the improvement in the time taken by M-QuadLTQP over DE-ANN based algorithm. Also M-QuadLTQP has better recall and precision for all other groups. Also, when these feature vectors are trained over proposed modified-CNN architecture, then they outperform all other state of the art techniques for all the groups. On adding CNN, the performance of M-quadLTQP features is improved in average up-to 4.7% and 0.8% in terms of ARR and ARP respectively.

It can be seen from Table 2 that M-QuadLTQP when used along with modified CNN performed 7.4%, 21.4% and 31.1% better than DE-ANN, DLTerQEP and LTP algorithm in terms of sensitivity. Further, an increase of 1.2%, 25.6% and 43.1% is also seen in terms of precision when compared with DE-ANN, DLTerQEP and LTP algorithms respectively.

Also as observed from TABLE 2, there is an improvement of 4.22%, 8.28% and 59.3% in terms of specificity over DE-ANN, DLTerQEP and LTP algorithm respectively. The ROC curve and AUC values are shown in Fig. 9 where it can be easily observed that the proposed M-QuadLTQP with modified CNN has highest AUC value and better ROC curves than all other algorithms.

The value of AUC obtained for M-QuadLTQP with modified CNN is 0.942 with TPR value as 0.911 and FPR as 0.944. The maximum number of epochs in the case of both datasets after which the results got stable is 8. Also around 250 iterations have been used to obtain these results.

Further the proposed method has been compared with the state of the art techniques in terms of accuracy in Table 3. There is an increase in accuracy for the proposed M-QuadLTQP is by 50.6%, 24.1% and 4.7% over LTP, DLTerQEP and DE-ANN techniques.

Fig. 10 XXXXX.

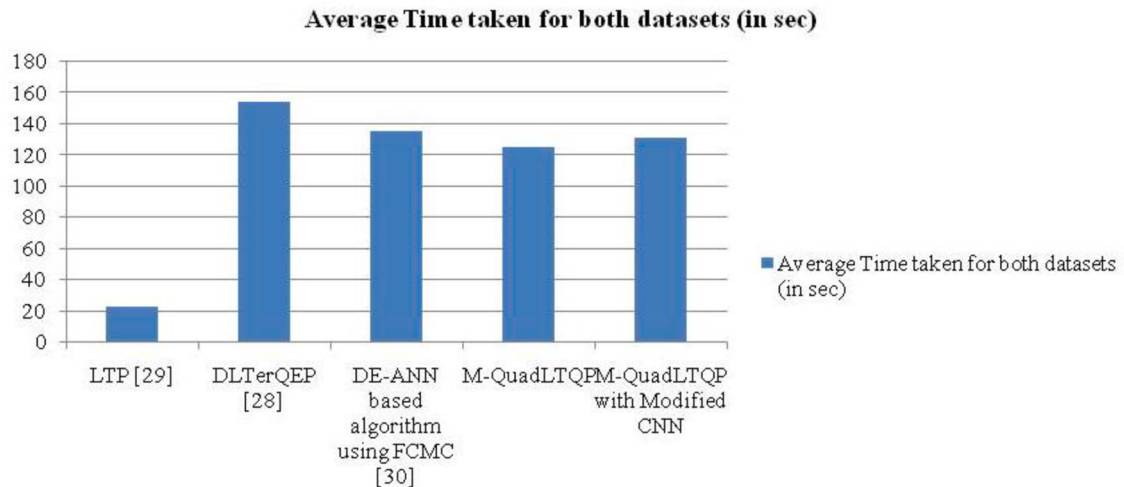


**Fig. 11.** Time taken by various algorithms for retrieval of skin cancer images for a single test case.

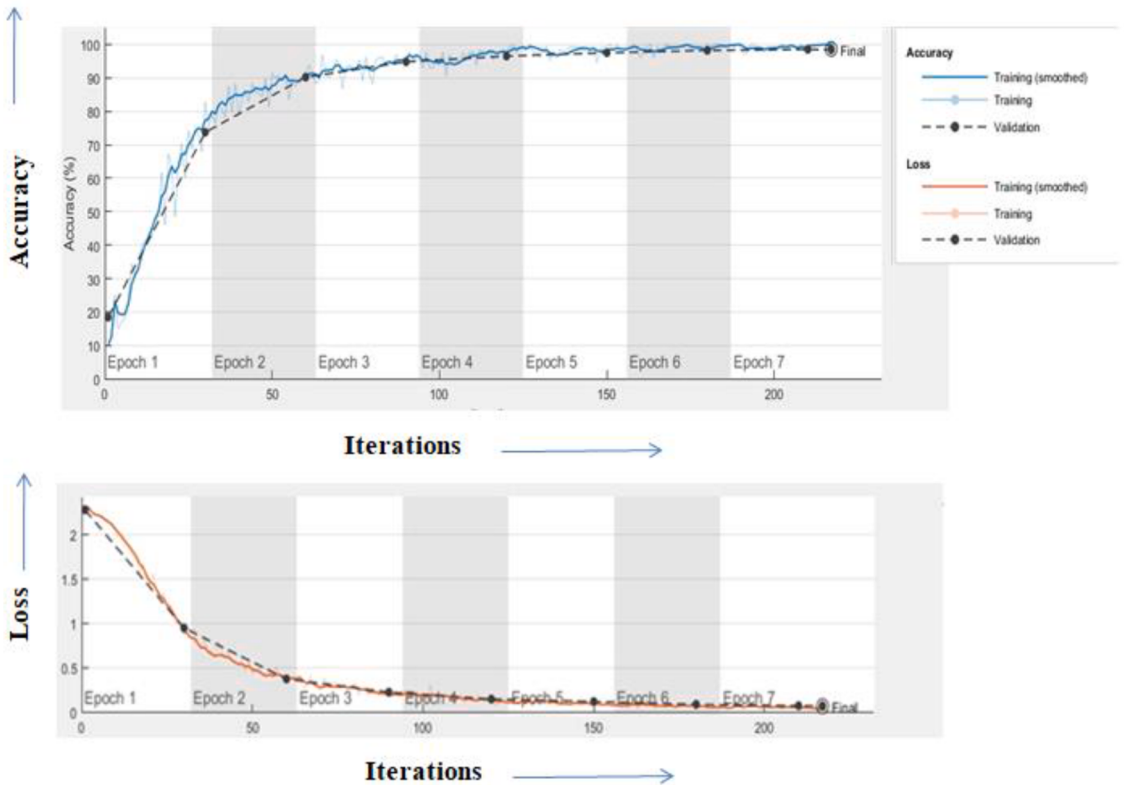


**Fig. 12.** Accuracy and loss of training and validation set for proposed algorithm on ISIC-UDA-1 dataset.

The comparison for the time taken in predicting the output class for a single test case or query image by various algorithms is given in Fig. 11.

The proposed feature set along with modified CNN takes less time than DE-ANN and DLTerQEP approaches for test case of a single observation. The time taken by LTP is lesser than M-QuadLTQP but the performance of M-QuadLTQP is much superior to LTP.

The variation of accuracy and loss with respect to the number of epochs for ISIC\_UDA-1 dataset is shown in Fig. 12 whereas for HAM10000 dataset it is shown in Fig. 13. The graph clearly shows that there is no drop in validation accuracy and hence there is no over fitting.

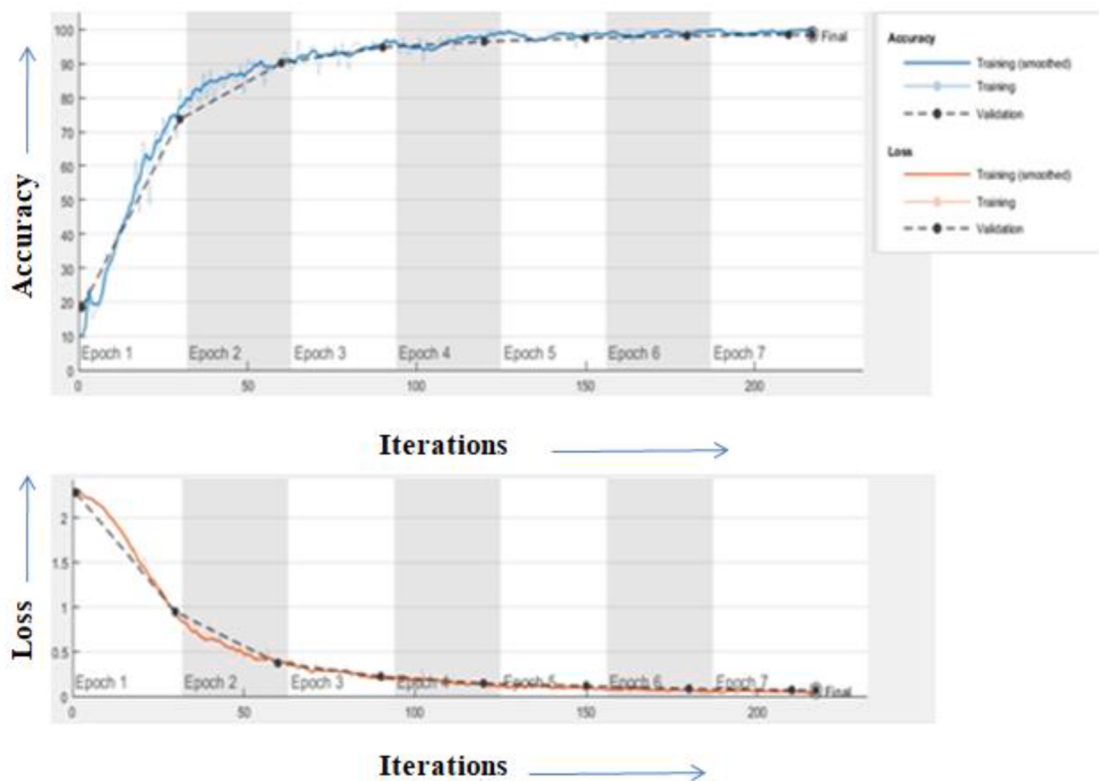


**Fig. 13.** Accuracy and loss of training and validation set for proposed algorithm on HAM10000 dataset.

**Table 1** and **Table 2** shows that there is an increase in average precision of the proposed methodology for two databases over LTP, DLTerQEP and DE-ANN approach by 36.86%, 21.08%, and 3.64%, increase in average specificity by 44.89%, 5.1%, and 10.1% and increase in average sensitivity for two databases by 20.88%, 15.07% and 5.60% respectively.

#### 4. Conclusion

In the given work, a texture based feature extraction technique; M-QuadLTQP is presented for the classification of dermatoscopic skin cancer images. The technique uses median based threshold and then extracts quantized LTP features in a unique manner from  $7 \times 7$  neighborhoods of a center pixel. The features are then used for training a modified CNN to classify different types of skin cancer or keratosis images. Use of a bigger neighborhood yields a more powerful feature vector with less noise. Also, the time taken by the algorithm is reduced drastically as compared to the existing deep learning based models. Multiple parameters like sensitivity, specificity, precision and accuracy are used to compare the proposed work with other state of the art techniques. The average accuracy proposed method is 96%, which is better than the previous established methods. Also an average increase in accuracy for these two publicly available datasets is more than 50%, 24% and 5% over Local Ternary Pattern, directional quantized extrema pattern and a differential evolution ANN inspired skin cancer detection approach.

#### Code availability

<https://github.com/varun0621/SkinCancer-Detection>.

#### Declaration of Competing Interest

Authors have no conflict of interest to declare.

#### Data Availability

Data will be made available on request.

## References

- [1] Suganyadevi S, Seethalakshmi V, Balasamy K. A review on deep learning in medical image analysis. *Int J Multimed Inf Retr* 2022;11(1):19–38.
- [2] Janda Monika, Olsen Catherine M, Cust Anne E. Early detection of skin cancer in Australia—current approaches and new opportunities. *Public Health Res Pract* 2022;32(1):3212204.
- [3] Fu Zexian, An Jing, Yang Qiuyu, Yuan Haojun, Sun Yuhang, Ebrahimian Homayoun. Skin cancer detection using Kernel Fuzzy C-means and developed red fox optimization algorithm. *Biomed Signal Process Control* 2022;71:103160.
- [4] Mishra Rosy, Meher Sushant, Kustha Nitish, Pradhan Tanuja. A skin cancer image detection interface tool using VLF support vector machine classification. *Computational intelligence in pattern recognition*. Singapore: Springer; 2022. p. 49–63.
- [5] Oukil S, Kasmi R, Mokrani K, García-Zapirain B. Automatic segmentation and melanoma detection based on color and texture features in dermoscopic images. *Skin Res Technol* 2022;28(2):203–11.
- [6] Durgarao Nagayalanka, Sudhavani Ghanta. Diagnosing skin cancer via C-means segmentation with enhanced fuzzy optimization. *IET Image Process* 2021.
- [7] Arora Ginni, Dubey Ashwani Kumar, Jaffery Zainul Abdin, Rocha Alvaro. Bag of feature and support vector machine based early diagnosis of skin cancer. *Neural Comput Appl* 2020;1–8.
- [8] Balaji M, Saravanan S, Chandrasekar M, Rajkumar G, Kamalraj S. Analysis of basic neural network types for automated skin cancer classification using Firefly optimization method. *J Ambient Intell Humaniz Comput* 2021;12(7):7181–94.
- [9] Patel B, Dhayal K, Roy S, Shah R. Computerized skin cancer lesion identification using the combination of clustering and entropy. In: 2017 international conference on big data analytics and computational intelligence (ICBDAC). IEEE; 2017. p. 46–51.
- [10] Ain QurratUl, Xue Bing, Al-Sahaf Harith, Zhang Mengjie. Genetic programming for multiple feature construction in skin cancer image classification. In: 2019 international conference on image and vision computing New Zealand (IVCNZ). IEEE; 2019. p. 1–6.
- [11] Maron RC, Schläger JG, Haggemüller S, von Kalle C, Utikal JS, Meier F, Gellrich FF, Hobelsberger S, Hauschild A, French L, Heinzerling L. A benchmark for neural network robustness in skin cancer classification. *Eur J Cancer* 2021;155:191–9.
- [12] Brinker TJ, Hekler A, Enk AH, Klode J, Hauschild A, Berking C, Schilling B, Haferkamp S, Schadendorf D, Fröhling S, Utikal JS. A convolutional neural network trained with dermatoscopic images performed on par with 145 dermatologists in a clinical melanoma image classification task. *Eur J Cancer* 2019;111:148–54. Apr 1.
- [13] Tschancli P, Rinner C, Apalla Z, Argenziano G, Codella N, Halpern A, Janda M, Lallas A, Longo C, Malvehy J, Paoli J. Human–computer collaboration for skin cancer recognition. *Nat. Med.* 2020;26(8):1229–34. Aug.
- [14] Nawaz Marriam, Mahmood Zahid, Nazir Tahira, Naqvi Rizwan Ali, Rehman Amjad, Iqbal Munwar, Saba Tanzila. Skin cancer detection from dermatoscopic images using deep learning and fuzzy k-means clustering. *Microsc Res Tech* 2022;85(1):339–51.
- [15] Brinker TJ, Hekler A, Enk AH, Klode J, Hauschild A, Berking C, Schilling B, Haferkamp S, Schadendorf D, Holland-Letz T, et al. Deep learning outperformed 136 of 157 dermatologists in a head-to-head dermatoscopic melanoma image classification task. *Eur J Canc* 2019;113:47–54.
- [16] Tschancli Philipp, Rosendahl Cliff, BenguNisaAkay Giuseppe Argenziano, Blum Andreas, Braun Ralph P, Cabo Horacio, et al. Expert-level diagnosis of nonpigmented skin cancer by combined convolutional neural networks. *JAMA Dermatol* 2019;155(1):58–65.
- [17] Chaturvedi Saket S, Gupta Kajol, Prasad Prakash S. Skin lesion analyser: an efficient seven-way multi-class skin cancer classification using mobilenet. In: *International Conference on Advanced Machine Learning Technologies and Applications*. Springer, Singapore; 2020. p. 165–76.
- [18] Kousis Ioannis, Perikos Isidoros, Hatzilygeroudis Ioannis, Virvou Maria. Deep learning methods for accurate skin cancer recognition and mobile application. *Electronics (Basel)* 2022;11(9):1294.
- [19] Kassam MA, Hosny KM, Fouad MM. Skin lesions classification into eight classes for ISIC 2019 using deep convolutional neural network and transfer learning. *IEEE Access* 2020;8:114822–32.
- [20] Jain S, Singhania U, Tripathy B, Nasr EA, Aboudaif MK, Kamrani AK. Deep learning-based transfer learning for classification of skin cancer. *Sensors* 2021;21(23):8142. Jan.
- [21] Tschancli P, Rosendahl C, Kittler H. The HAM10000 dataset, a large collection of multi-source dermatoscopic images of common pigmented skin lesions. *Sci. Data* 2018;5:180161.
- [22] D. Gutman, N.C. Codella, E. Celebi, B. Helba, M. Marchetti, N. Mishra, A. Halpern, Skin Lesion Analysis Toward Melanoma Detection: a Challenge at the International Symposium on Biomedical Imaging (ISBI) hosted by the International Skin Imaging Collaboration (ISIC), 2016.
- [23] Deep G, Kaur L, Gupta S. Directional local ternary quantized extrema pattern: a new descriptor for biomedical image indexing and retrieval. *Eng Sci Technol Int J* 2016;19(4):1895–909. Issue.
- [24] Tan X, Triggs B. Enhanced local texture feature sets for face recognition under difficult lighting conditions. *IEEE Trans Image Process* 2010;19(6):1635–50. Issue.
- [25] Kumar Manoj, Alshehri Mohammed. "A de-ann inspired skin cancer detection approach using fuzzy c-means clustering. *Mobile Netw Appl* 2020;25:1319–29.

Varun Srivastava: He is working as an assistant professor in Department of Computer science at TIET Patiala, India. He has done his doctorate in the field of Biomedical Image processing from GGSIPU Delhi. He is an author of more than 20 publications in refereed international journals and conferences. His-fields of interests include biomedical image processing, and machine learning.

Deepika Kumar: She is working as an assistant professor in Bharati Vidyapeeth's College of Engineering. He is an author of more than 30 publications in refereed international journals and conferences. His-fields of interests include Deep learning, Data science and machine learning.

Sudipta Roy: He is working as an assistant professor at Jio Institute, India. He is an author of more than 50 publications in refereed international journals and conferences. In recognition of his exceptional contributions to the IEEE access, Editorial Office honoured him as an Outstanding Associate Editor. His-fields of research interests are image processing, artificial intelligence, and machine learning.